Crystal Structure of Poly(2-cyano-1,4-phenylene terephthalamide)

Soo-Young Park,*,† Seung-Woo Lee,† Tae-Jin Oh,‡ and John Blackwell§

Department of Polymer Science and Department of Dyeing and Finishing, Kyungpook National University, #1370 Sankyuk-dong, Buk-gu, Daegu 702-701, Korea, and Department of Macromolecular Science, Case Western Reserve University, Cleveland, Ohio 44106

Received January 25, 2005; Revised Manuscript Received February 15, 2005

ABSTRACT: The crystal structure of poly(2-cyano-1,4-phenylene terephthalamide) (CN-PPTA) has a monoclinic (metrically orthorhombic) unit cell with dimensions $a = 9.21$ Å, $b = 5.08$ Å, and $c = 12.9$ Å, containing monomer repeats of two chains. The space group is $P2_1/n$, and the two chains in the unit cell are related by both the n-glide plane and the 2_1 screw axis. The calculated density is 1.447 g/mL, which is close to the observed density of 1.420 g/mL. A number of models were considered to accommodate the random 50/50 −CN substitution at 2- and 3-positions of the *p*-phenylenediamine segment. The data favor a structure in which 3-CN-substituted phenylenes are rotated by 180° (about their 1,4-axes), so that effectively we have a mixture of 2- and 5-CN groups, which allows the substituents on adjacent chains to interleave. This structure would in fact be compatible with 2,5-disubstitution: random monosubstitution was modeled by 50% occupancy for the atoms of the −CN groups. LALS refinement led to a structure free of steric hindrance, with a crystallographic R value was 0.27. The phenylene−amide torsion angles are 50° for the *p*-phenylenediamine segment and −30° for the terephthalic segment, values which are similar to those seen for Kevlar. The amide plane is rotated from the *bc* plane of the unit cell by 11°. The density is lower than that observed for Kevlar (1.50 g/mL) due mainly to the 50% vacancies at the CN sites. These vacancies probably facilitate penetration of the lattice by common polar organic molecules, leading to higher solubility.

Introduction

Fibers of poly(*p*-phenylene terephthalamide) (PPTA; DuPont Kevlar) has excellent thermal and thermoxidative stability as well as exceptional tensile strength and tensile modulus. These properties are attributable to the chain stiffness and the high degree of molecular orientation and crystallinity, which are achieved by dry jet wet spinning from a liquid crystalline solution of PPTA in hot 100% sulfuric acid.[1−4] However, the use of sulfuric acid as the solvent results in some molecular weight degradation, and thus to less than optimum physical properties, and also leads to difficulties in environmental and process control. Chemical modification of PPTA in order to improve the solubility has been attempted, e.g., by adding halogens or other chemical substituents on the phenylene rings.[5] In the present paper we will address the structure of one such modification: poly(2-cyano-1,4-phenylene terephthalamide) (CN-PPTA), in which a cyano group is substituted at the *p*-phenylenediamine segment. This polymer is soluble in polar organic solvents that contain a small amount of inorganic salts; an example is dimethylacetamide (DMAc) containing 2% LiCl/DMAc.[6,7] The tensile strength and modulus of the CN-PPTA fibers spun in the lyotropic state are comparable with those of Kevlar, even though bulky cyano groups have been substituted.[6,7]

We have investigated the crystal structure of CN-PPTA fibers by X-ray diffraction, LALS refinement,[16,17] FT-IR,[11−13] and molecular modeling,[18−21,27] in an effort to understand the origin of higher solubility as compared to that of Kevlar. The crystal structure and properties of unsubstituted PPTA have been studied by a number of physical chemical techniques, including wide-angle X-ray diffraction,[8,9] transmission electron microscopy,[10] FT-IR,[11−13] and atomistic molecular modeling.[4,5,10] Northolt[14] interpreted the X-ray fiber pattern in terms of a monoclinic (metrically orthorhombic) unit cell with dimensions $a = 7.87$ Å, $b = 5.18$ Å, and $c = 12.9$ Å, and space group Pn. The unit cell contained monomer segments of two chains: the center chain is related to the corner chain by an n-glide plane at $z = 1/2c$. The torsion angles between the phenylene and amide planes are 38° for the *p*-phenylenediamine segment and −30° for the terephthalic segment.[14] Contiguous chains in the *010* plane are linked by C═O···H−N hydrogen bonds. Tadokoro et al.[15] independently proposed a similar structure in which the space group is $P2_1/n$. The Pn structure of Northolt differs from that proposed by Tadakoro by a small axial shift of 0.32 Å. Liu et al.[10] proposed a similar crystal structure in which the unit cell is monoclinic with dimensions $a = 7.88$ Å, $b = 5.22$ Å, c (unique) = 12.9 Å, and $\gamma = 90°$ and space group Pa based on electron diffraction PPTA prepared by confined thin film melt polymerization. However, most structural discussions have been in terms of the Pn and $P2_1/n$ models,[4,5] which will be the starting point for our studies of CN-PPTA.

Experimental Section

Materials. CN-PPTA was synthesized as described in a US patent.[22] Fibers were spun from the lyotropic liquid crystalline phase of the polymer by dry jet wet spinning, using a custom-made device.[23] An anisotropic CN-PPTA dope (13 wt % polymer in *N*-methylpyrrolidone containing 5 wt % LiCl) was deaerated at 50 °C and filtered through a 74 mm stainless steel mesh.[6,7] Fibers were spun at 50 °C with a draw ratio of 10 into a 1 cm air gap before entering a distilled water coagulation bath maintained at 5 °C. These fibers were washed in a large excess

---

[†] Department of Polymer Science, Kyungpook National University.

[‡] Department of Dyeing and Finishing, Kyungpook National University.

[§] Case Western Reserve University.

[*] To whom correspondence should be addressed: Tel +82-53-950-5630; Fax +82-53-950-6623; e-mail psy@knu.ac.kr.

10.1021/ma050161t CCC: $30.25

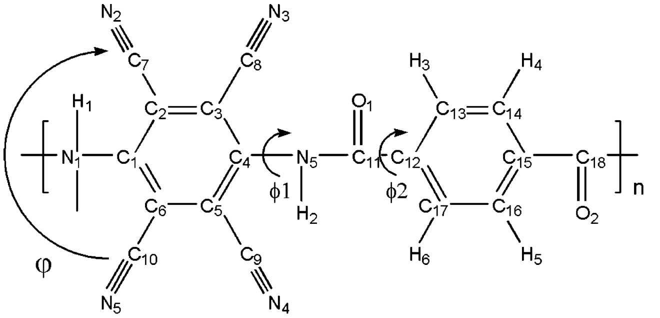

Figure 1. Chemical structure and atomic numbering for the model of the CN-PPTA monomer: ϕ_1 and ϕ_2 are the $C_3-C_4-N_6-C_{11}$ and $N_6-C_{11}-C_{12}-C_{13}$ torsion angles; the rotational angle φ is the angle between the *bc* plane of the unit cell and the planar amide groups.

of distilled water for several days to remove residual solvent, air-dried fiber, and then heat-treated at 400 °C for a few seconds.

X-ray Diffraction. Wide-angle X-ray diffraction patterns were recorded on a phosphor image plate (Molecular Dynamics) using a Statton camera (pinhole collimation) and graphite-crystal-monochromated Cu Kα radiation from a rotating anode X-ray generator operating at 40 kV and 240 mA. The specimen-to-film distance was calibrated using SiO_2 powder. The integrated intensities of 16 observed reflections were measured using FIT2D software.[20] A reflection with a maximum at 2θ (Bragg angle) and ζ (azimuthal angle) was integrated azimuthally within angular limits (ζ_1, ζ_2) that defined the edges of the reflection, yielding a plot of intensity (I) vs 2θ. A linear background (between the inner and outer edges of the reflection, $2\theta_1$, $2\theta_2$) was subtracted, and the intensity $I(hkl)$ was determined by integration. Partially overlapped reflections were separated by curve fitting of Gaussian functions. The structure factor $F(hkl)$ was calculated after multiplicity, Lorenz, and polarization corrections.[24–26]

Density. The density was measured in a density gradient column prepared by mixing toluene and carbon tetrachloride, calibrated with standard density balls.

Molecular Modeling. Molecular modeling and simulation of the X-ray patterns were carried out using Cerius2 software.[21] The conformational energy was calculated ab initio using the Gaussian 98 program[27] at the Hartree–Fock[18,19] 6-31G** level.

Figure 1 shows the chemical structure of CN-PPTA and the numbering of the atoms to be used in the text. There are four possible positions for the $-CN$ group on the *p*-phenylenediamine segment. Random disposition of the $-CN$ group was treated by assigning fractional occupancies. The bond lengths and bond angles were those used in the Northolt model of Kevlar,[14] and the phenylenes and amide groups were assumed to be planar. For the linear $-CN$ group, $C-N = 1.16$ Å, $C_{aromatic}-C = 1.44$ Å, and $C_{aromatic}-C_{aromatic}-C = 120°$. The backbone torsion angles, ϕ_1 and ϕ_2, are the angles between the amide planes and the adjacent *p*-phenylenediamine and terephthalic units, respectively; $\phi_1 = \phi_2 = 0°$ corresponds to the planar conformation shown in Figure 1. The orientation of the chains within the unit cell is defined by the chain rotational angle φ, the angle between the *bc* plane of the unit cell and the coplanar amide groups; $\varphi = 0°$ when the plane of the amide group is parallel to the *bc* plane. Positive angles correspond to clockwise rotation.

Refinement. Structural refinement was performed by using WinLALS software[16,17] with the bond lengths and bond angles constrained to those reported for Kevlar.[14] The parameters refined were the rotation angle φ, torsion angles ϕ_1 and ϕ_2, an isotropic temperature factor B_{iso}, and a scale factor to normalize the total observed and calculated $F^2(hkl)$.[26,28]

Fourier Transform Infrared Spectroscopy. FT-IR spectra were recorded using a JASCO FT/IR 620 spectrometer. The specimens were 10 mm diameter KBr pellets containing 5×10^{-2} wt % of ground CN-PPTA. Spectra were derived from 50 coadded interferograms obtained at a resolution of 1 cm^{-1}.

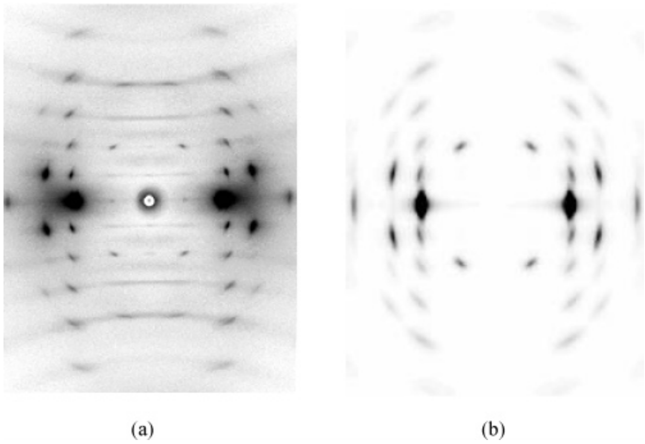

(a) (b)

Figure 2. (a) X-ray fiber diagram for CN-PPTA fibers. (b) Simulated X-ray fiber diagram for model 2 (Table 2), with crystal size 100 Å, and the full width of the half-maximum of the azimuthal scanning was 3°.

Table 1. Observed *d* Spacings (d_o) and Structure Factors (F_o) for the 16 Reflections in the Fiber Diagram of CN-PPTA Compared to the Calculated Data for Model 2

h	*k*	*l*	2θ	d_o (Å)	d_c (Å)	F_o	F_c
1	0	0	9.49	9.21	9.22	9.40	0.00
2	0	0	18.81	4.74	4.60	162	181
1	1	0	19.89	4.45	4.44	155	159
3	1	0	33.49	2.67	2.63	107	119
1	1	1	21.05	4.21	4.20	64.3	51.8
2	1	1	26.72	3.33	3.29	154	115
1	0	2	16.56	5.34	5.29	23.5	28.5
2	0	2	23.32	3.81	3.75	29.3	24.5
1	1	2	24.21	3.67	3.66	42.8	33.1
2	1	2	28.87	3.09	3.01	11.6	37.9
1	1	3	28.80	3.09	3.09	67.9	29.2
2	1	3	33.11	2.70	2.67	32.8	47.7
1	0	4	29.10	3.06	3.05	34.8	19.0
2	0	4	33.57	2.66	2.64	26.6	36.3
1	1	4	34.27	2.61	2.61	46.5	35.0
1	1	5	40.22	2.24	2.23	47.5	39.2

Results and Discussion

X-ray Fiber Patterns. Figure 2a shows the X-ray fiber pattern for CN-PPTA; the fiber axis is vertical. The data are indicative of high crystallinity and orientation: the Herman's orientation factor[24] is 0.98 based on the azimuthal scanning of the *200* reflection; the full width at the half-maximum for a 2θ scan of the same reflection yields a lateral crystallite size of 100 Å. The streakiness of the layerlines indicates the amorphous regions are largely oriented chains lacking three-dimensional register. Sixteen Bragg reflections are resolved, with *d* spacings listed in Table 1, and are indexed by a metrically orthorhombic unit cell with dimensions $a = 9.21$ Å, $b = 5.08$ Å, and $c = 12.9$ Å, based on least-squares refinement. The calculated *d* spacings are given in Table 1 and are in good agreement with those observed. The discrepancy for the *200* reflection suggests the presence of some lateral disorder. The calculated density is 1.447 g/mL with monomeric units of two chains in the unit cell, which is close to the measured density of 1.420 g/mL.[6,7] The *b* dimension (5.08 Å) of CN-PPTA is a little less than that for Kevlar (5.18 Å) but suggests that there are similar $C{=}O\cdots H-N$ hydrogen-bonds along that direction.[14,15]

The presence of a weak *100* reflection as well as the strong *200* and *110* reflections indicates that the chains

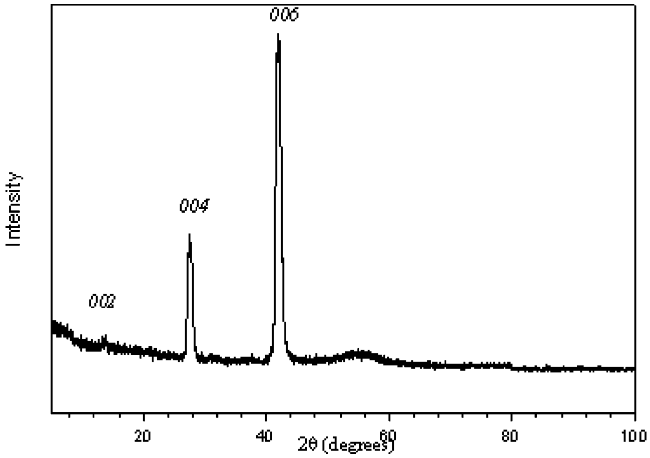

Figure 3. $\theta/2\theta$ diffractometer scan of CN-PPTA along the fiber axis.

are disposed only approximately at the corner and center of the *ab* projection: *100* would be absent if this symmetry was exact.

Figure 3 shows a $\theta/2\theta$ diffractometer scan along the fiber axis direction in which we see the *00l* reflections which are not visible in the X-ray fiber pattern on account of the orientation. The reflections at $2\theta = 13.9°$ ($d = 6.38$ Å), 28.7° ($d = 3.21$ Å), and 45.9° ($d = 2.15$ Å) can be indexed as 002, 004, and 006, respectively. The absence of 001, 003, and 005 reflections indicate that the two chains in the crystal are shifted away from each other by approximately $c/2$. The repeat distance along the chain axis (c dimension) is 12.9 Å, the same as that of Kevlar.[14,15] It is interesting to note that the *008* reflection is not detectable.

Space Group. Systematic absences occur for the *hk0* ($h + k =$ odd) and *h0l* ($l =$ odd) reflections, except that a weak *100* reflection is detected; the presence of the latter reflection is probably due to distortions, as will be discussed later. The same systematic absences are observed for Kevlar,[14,15,29] consistent with the two possible space groups, Pn and $P2_1/n$.[14,15] Both space groups have n-glide planes perpendicular to the chain axis. The main difference these two space groups is in the position of the glide plane: for $P2_1/n$ it passes though the center of the amide group, halfway between the two phenylene rings, whereas Pn permits a shift in the glide plane shift along the c-axis. Northolt[14] originally proposed a $P2_1/n$ space group but obtained better agreement with the observed intensities, particularly for the meridional and near-meridional reflections (e.g., *006*, *004*, *106*, *104*, and *105*), by introducing a small (0.32 Å) shift of the second chain along the c-axis, reducing the symmetry to Pn.[14]

In space group $P2_1/n$, the equivalent positions are (1) x, y, z, (2) $-x + {}^1/_2, -y + {}^1/_2, z + {}^1/_2$, (3) $-x, -y, -z$, (4) $x - {}^1/_2, y - {}^1/_2, -z - {}^1/_2$.[29] There are centers of symmetry at 0, 0, 0 and ${}^1/_2, {}^1/_2, {}^1/_2$, 2_1 screw axes parallel to c at $x = {}^1/_4$, $y = {}^1/_4$, and $x = {}^3/_4$, $y = {}^3/_4$, and n-glide planes parallel to ab at $z = 0$ and $z = {}^1/_2$. Thus, the chains have centers of symmetry at the centers of the phenylenes, and the second chain is generated by a 180° rotation about z and a shift of $z = {}^1/_2$; the glide plane passes through the amide group, halfway between the centers of the phenylenes. However, when the symmetry is reduced to Pn, the position of the glide plane is changing the origin in the chain. In Pn, the general coordinates of the two chains are (1) x, y, z and (2) $x + {}^1/_2, y + {}^1/_2, -z$.[29] Thus, the shift between the chains is not limited to $z = {}^1/_2$, and *00l* reflections with $l =$ odd can occur, and their intensity will depend on the magnitude of the shift. Only 00l with $l =$ even reflections are observed in Figure 3, indicating that any deviations from $P2_1/n$ are likely to be small. Nevertheless, the structure was refined using the less symmetrical Pn space group.

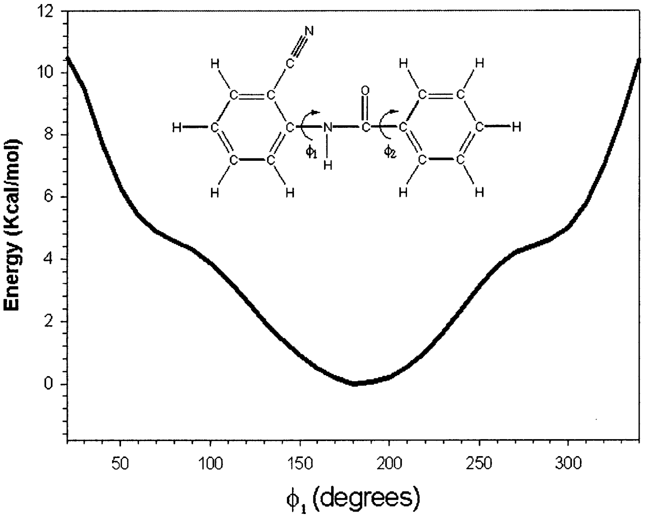

Figure 4. Conformational energy of CN-PPTA with the fixed $\phi_2 = -30°$ using the ab initio method (HF, 6G-31** basis) of Gaussian 98. The structure in the inset is for $\phi_1 = 0°$.

Models. In view of the synthesis route one expects a random microstructure for CN-PPTA; i.e., the $-$CN groups are substituted randomly, and there is no evidence for a preference for one or more positions on the phenylenediamine. If the backbone has a center of symmetry in the center of the phenylene, substituents at C3 or C6 would have the same environment, as would substituents at C2 or C5. Before refining against the X-ray data, we compared three basic models in terms of their potential energies. In model 1, CN groups are randomly disposed (50/50) at C3 and C6; in model 2, they are randomly disposed at C2 and C5; in model 3, there is completely random substitution, i.e., 25% at each of C2, C3, C4, and C5. With the substituents treated as fractional occupants, models 1−3 remain centrosymmetric. Model 1 can be converted to model 2 by a 180° rotation at torsion angle ϕ_1 but is considered separately for packing purposes. We also examined nonsymmetric models: in model 4 the substituents are 50/50 at C2 and C3; in model 5 they are 50/50 at C5 and C6, so that in both cases they are always on one side of the molecule. Model 6 is the extreme case: all the substituents at the same position, C2, in which case the chain has a sense, so that parallel and antiparallel packings needed to be considered. However, simulated X-ray patterns for the structures constructed using models 5−7 contained many unobserved reflections as a result of the lack of the symmetry, and only models 1−3 needed to be considered further.

If the amide and phenylene units are assumed to be planar, the conformation of the backbone is defined by the two torsion angles ϕ_1 and ϕ_2. Figure 4 shows the ab initio conformational energy of phenylbenzamide vs ϕ_1. (ϕ_2 was set at −30°, as in the structure of Kevlar, because the presence of the −CN group on the opposite phenyl has little effect on this conformational angle.) The structure in the inset is for $\phi_1 = 0°$. The conformational energy is almost symmetrical about the minimum

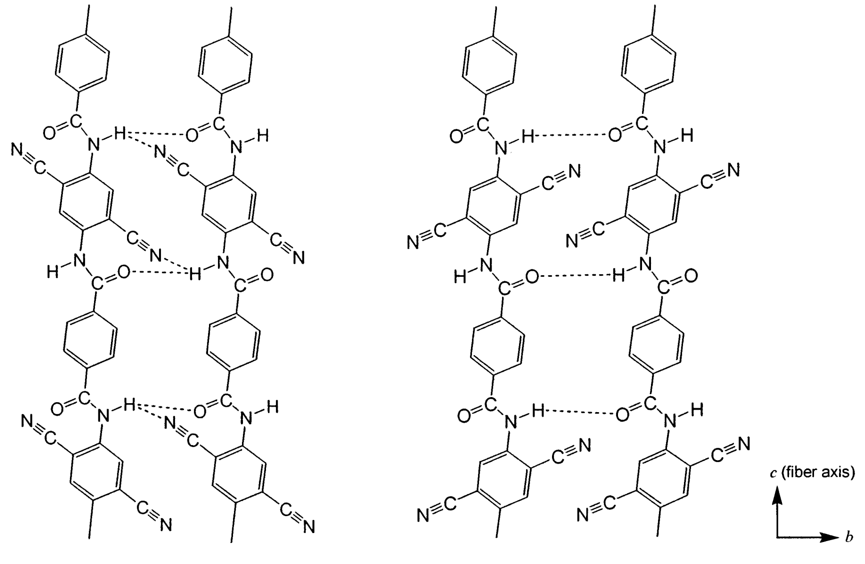

(a) (b)

Figure 5. Schematics of the *bc* plane of the structure of CN-PPTA constructed with (a) model 1 and (b) model 2 for the chain. The dashed lines represent the predicted hydrogen bonds.

at $\phi_1 = 180°$. (The asymmetry is due to setting $\phi_2 = -30°$ rather than 0°, and the small effect indicates that even with the substituent present, the minimum for ϕ_1 is not highly dependent on ϕ_2.) The structure at $\phi_1 = {\sim}0°$ describes the amide···CN interactions in model 1; $\phi_1 = {\sim}180°$ corresponds to the situation in model 2.

Given the similarity of the unit cell to that for unsubstituted Kevlar, the structure is likely to contain layers of chains linked by C=O···H−N hydrogen bonds, for which the phenylene−amide planes will need to be inclined by ~30°. The energy at $\phi_1 = {\sim}30°$ is 8.8 kcal/mol higher than for $\phi_1 = {\sim}150°$ (180° − 30°) due to the steric interaction between the −CN and C=O groups, strongly favoring model 2.

The crystal structure of Kevlar[14,15] was adapted to construct initial models for the crystal structure of CN-PPTA, allowing for the dilated unit cell to accommodate the −CN groups. Figure 5 shows the *bc* plane of these models of CN-PPTA and the hydrogen bonds (dotted lines) predicted by Cerius2.[21] In model 2 (Figure 5b) we have the C=O···H−N bonds as in Kevlar; in model 1 (Figure 5a) the situation is more complex due to the proximity of the −CN group, requiring bifurcated (three-center) hydrogen bonding[30] of N−H to O=C and N≡C. The latter type of the hydrogen bonding has not yet been reported to our knowledge. Model 3 is also unfavorable because 50% of the −CN groups would be arranged as in model 1.

Figure 6 shows the FT-IR spectra of Kevlar, CN-PPTA, and benzonitrile. The peaks at 3320 cm^{-1} for CN-PPTA and Kevlar are assigned to N−H stretching vibration of the hydrogen-bonded *trans*-amide[11−13] and suggests the same kind of C=O···H−N bonding. The peak at 2230 cm^{-1} for CN-PPTA assigned to the −C≡N stretching vibration[11−13] compares well with that at 2229 cm^{-1} for benzonitrile and suggests that the −CN group is not involved in hydrogen bonding. These data suggest that model 2, which can form the same −C=O and −N−H as in Kevlar, is the more likely basis for the crystal structure of CN-PPTA. The amide I mode occurs at 1658 cm^{-1} for CN-PPTA, higher than the 1646 cm^{-1} observed for Kevlar, suggesting that the steric requirements for incorporation of the −CN groups lead to a slightly longer hydrogen bond. This is consistent the higher solubility of CN-PPTA in common polar organic solvents.

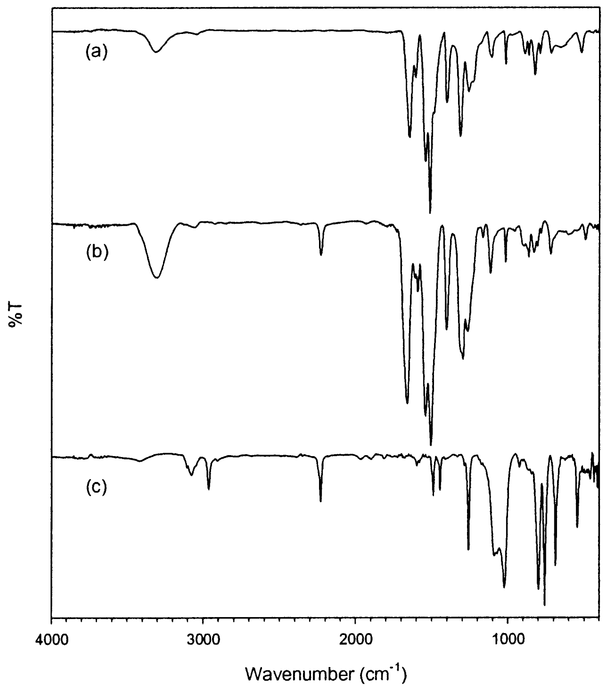

Figure 6. FT-IR spectra of (a) Kevlar, (b) CN-PPTA, and (c) benzonitrile.

Table 2. Refined Parameters for CN−PPTA (Model 2)

φ (deg)	11.10	ϕ_2 (deg)	27.75
B_{iso} (Å^2)	0.44	R (%)	27.32
ϕ_1 (deg)	−48.07		

Refinement. WinLALS refinement of model 2 with space groups *Pn* and $P2_1/n$ led to structures that were not significantly different, with $R = 27\%$. The refined parameters for the $P2_1/n$ structure are given in Table 2, and the atomic coordinates are in Table 3. A simulated X-ray fiber pattern for this structure generated

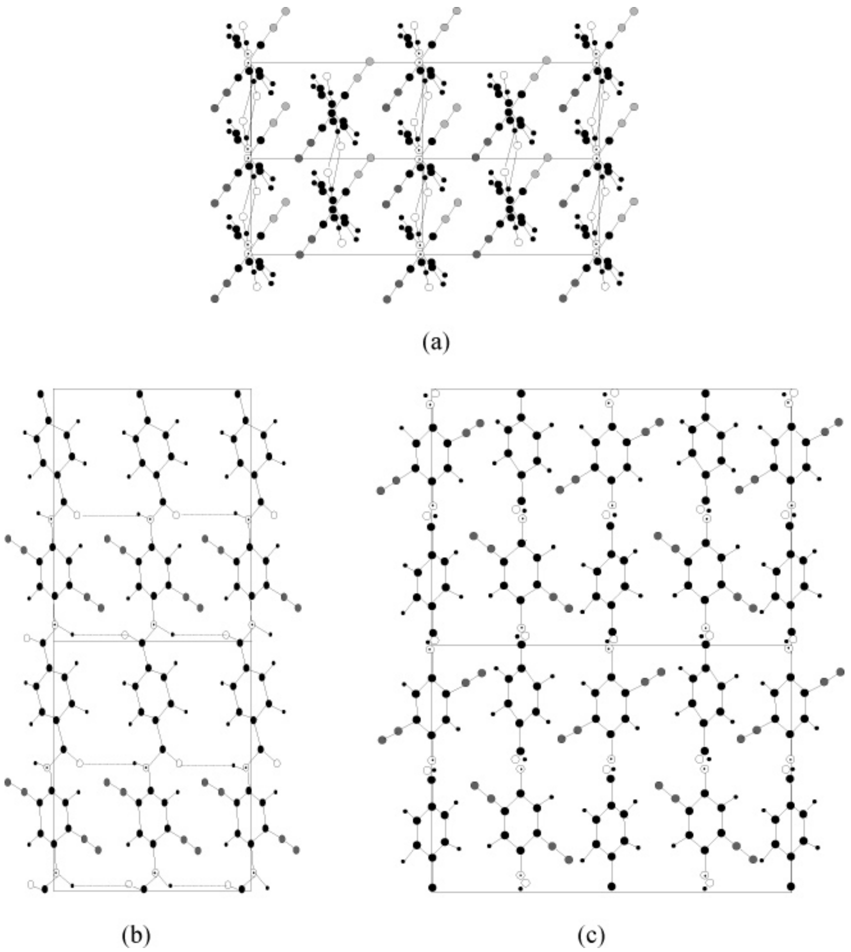

Figure 7. (a) *ab*, (b) *ac*, and (c) *bc* projections of the CN-PPTA model. The second hydrogen sheet was omitted for the clear view of the hydrogen bonding in (c).

Table 3. Cartesian Atomic Coordinates for the Refined Model 2

atom	*X*	*Y*	*z*
N1	0.0571	−0.2768	15.6752
H1	0.2480	−1.2015	3.1261
C1	0.0282	−0.1364	14.2564
C2	−0.7243	−1.0102	13.4893
C3	−0.7525	−0.8739	12.1113
C4	−0.0281	0.1362	11.5004
C5	0.7244	1.0100	12.2675
C6	0.7525	0.8737	13.6455
C7	−1.4775	−2.0605	14.1244
C9	1.4775	2.0602	11.6324
N2	−2.0842	−2.9065	14.6361
N4	2.0842	2.9062	11.1207
H8	−1.2958	−1.5048	11.5575
H10	1.2959	1.5046	14.1994
N5	−0.0571	0.2766	10.0817
H2	−0.2415	1.1696	9.6712
C11	0.1476	−0.7151	9.2086
O1	0.3832	−1.8562	9.6151
C12	0.0714	−0.3459	7.7784
C13	0.7529	−1.0940	6.8328
C14	0.6815	−0.7482	5.4936
C15	−0.0713	0.3456	5.1000
C16	−0.7528	1.0937	6.0456
C17	−0.6814	0.7480	7.3848
H3	1.2965	−1.8837	7.1170
H4	1.1735	−1.2883	4.8108
H5	−1.2964	1.8835	5.7614
H6	−1.1735	1.2881	8.0676
C18	−0.1476	0.7149	3.6698
O2	−0.3883	1.8809	3.3456

using Cerius2 with a crystallite size of 100 Å and orientation factor 3° is shown in Figure 2b and compares well with the observed data (Figure 2a). The observed and calculated structure factors are compared in Table 1. The *00l* reflections were not included in the refinement, but the calculated intensities for the *002*, *004*, and *006* reflections are in good agreement with those observed.

The 27% *R* value is relatively high when compared to the results for homopolymers, but this is probably due to inherent disorder in a structure with random substituents. The value of $\phi_1 = 48 \pm 2°$ is higher than in the structure of Kevlar (∼38°) as a result of the need to pack the bulky −CN groups. The value of $\phi_2 = 28 \pm 2°$ is similar to that for Kevlar (∼30°), confirming the modeling results indicating that the −CN substituent does not have much effect on the conformation at the terephthalate unit. The chain rotation $\varphi = 11°$ is larger than in Kevlar (∼4°), but the N···O hydrogen bond length is unaffected (3.01 Å vs 3.04 Å in Kevlar) as a consequence of the decreased *b* dimension (5.08 Å vs 5.18 Å in Kevlar). The N−H···O angle (145° vs 160° in Kevlar) is consistent with a slight weakening of the hydrogen bond, as indicated by the amide I mode.

Figure 7 shows *ab*, *ac*, and *bc* projections of the crystal structure. In the *ab* projection, the hydrogen bonds are inclined at ∼11° to the *b* axis, and the −CN groups are in the *310* plane. The "interleaving" of the −CN groups on adjacent chains is apparent in the *ac* projection: rotation about the linkage bonds makes it possible for the CN groups to be exclusively in the 2- and 5-positions, whereas the 3- or 6-positions would result in serious overlap. The chains are not in contact along the *a* axis, and there is additional "empty space" since only 50% of the −CN sites are occupied. The crystal structure of CN-PPTA is quite similar to that of Kevlar,[14,15] except for the −CN substituents. The vacant space accounts for the lower density, and probably facilitates solvent penetration, such that CN-PPTA is soluble in common organic solvents.

The observed weak *100* reflection is forbidden in space groups $P2_1/n$ (*hk0* absent for $h + k =$ odd) and suggests that there are small deviations from the symmetrical structure. When we introduced a small shift (δ) of the center chain along the a direction (to $a/2 + \delta$), we found that a 100 reflection with intensity comparable to that observed was generated with δ as small as 0.025 Å, which had negligible effect on the other intensities. There is no reason to expect such a shift in model 2, but at the edges of the crystallites, where the −CN groups may be preferentially on one side of the chain.

Conclusions

The crystal structure of poly(2-cyano-1,4-phenylene terephthalamide) (CN-PPTA) has been determined by winLALS refinement against wide-angle X-ray intensity data. The observed d spacings are indexed by a monoclinic (metrically orthorhombic) unit cell with dimensions $a = 9.21$ Å, $b = 5.08$ Å, and $c = 12.9$ Å with space group of $P2_1/n$, in which two chains in the unit cell are related by both the n-glide plane and 2_1 crew axis symmetries. Each chain is centrosymmetric, and the glide plane is perpendicular to the chain axis at the center of symmetry. The data are completely consistent with randon 2- and 3-substitution. The 3-substituted phenylenes are rotated about 180° (about their 1,4-axes), so that effectively we have a mixture of 2- and 5-CN groups, which allows the substituents on adjacent chains to interleave. This structure would in fact be compatible with 2,5-disubstitution, and random monosubstitution was modeled by 50% occupancy for the atoms of the −CN groups. The density is lower than that observed for Kevlar (1.50 g/mL) due mainly to the 50% vacancies at the CN sites. These vacancies probably facilitate penetration of the lattice by common polar organic molecules, leading to higher solubility.

Acknowledgment. This work was supported by Grant R08-2003-000-10338-0(2003) from the Basic Research Program of the Korea Science & Engineering Foundation and Brain Korea 21 program. We appreciate Prof. Kenji Okuyama (Tokyo University of Agriculture and Technology) for the fruitful discussions and supplying the winLALS program.

References and Notes

(1) Rebouillat, S.; Peng, J. C. M.; Donnet, J. B. *Polymer* **1999**, *40*, 7341.
(2) Rebouillat, S.; Donnet, J. B.; Wang, T. K. *Polymer* **1997**, *38*, 2245.
(3) Socci, E. P.; Thomas, D. A.; Eby, R. K.; Grubb, D. T.; Adams, W. W. *Polymer* **1996**, *37*, 5005.
(4) Park, S. J.; Seo, M. K.; Ma, T. J.; Lee, D. R. *J. Colloid Interface Sci.* **2002**, *252*, 249.
(5) Bair, T. I.; Morgan, P. W.; Killian, F. L. *Macromolecules* **1977**, *10*, 1396.
(6) Oh, T. J.; Han, S. J.; Kim, S. G. *J. Korean Fiber Soc.* **1996**, *33*, 814.
(7) Oh, T. J.; Jang, Y. S. *J. Korean Fiber Soc.* **1998**, *35*, 182.
(8) Rao, Y.; Waddon, A. J.; Farris, R. J. *Polymer* **2001**, *42*, 5937.
(9) Ran, S.; Fang, D.; Zong, X.; Hsiao, B. S.; Chu, B.; Cunniff, P. M. *Polymer* **2001**, *42*, 1601.
(10) Liu, J.; Cheng, S. Z. D.; Geil, P. H. *Polymer* **1996**, *37*, 1413.
(11) Tascon, J. M. D.; Mosquera, M. E. G.; Jamond, M.; Martinez-Alonso, A. *Chem. Mater.* **1994**, *6*, 1918.
(12) Minagawa, M.; Miyano, K.; Takahashi, M.; Yoshii, F. *Macromolecules* **1988**, *22*, 2387.
(13) Downing, J. W.; Newell, J. A., Jr. *J. Appl. Polym. Sci.* **2004**, *91*, 417.
(14) Northolt, M. G. *Eur. Polym. J.* **1974**, *10*, 799.
(15) Tadokoro, H.; Tashiro, K.; Kobayashi, M. *Macromolecules* **1977**, *10*, 413.
(16) Arnott, S.; Wonacott, S. *Polymer* **1966**, *7*, 157.
(17) Smith, P. J. C.; Arnott, S. *Acta Crystallogr., Sect. A* **1978**, *34*, 3.
(18) Irwin, R. S.; Vopagel, E. R. *Macromolecules* **1993**, *26*, 3391.
(19) Vargas, R.; Garza, J.; Dixon, D.; Hay, B. P. *J. Phys. Chem. A* **2001**, *105*, 774.
(20) www.esrf.fr/computing/scientific/FIT2D.
(21) www.accelrys.com.
(22) Oh, T. J. U.S. Patent (to Kolon), 5,728,799. 1995.
(23) Blades, H. U.S. Patent, 3,767,756. 1973.
(24) Alexander, L. E. *X-ray Diffraction Methods in Polymer Science*; John Wiley & Sons: New York, 1969.
(25) Okuyama, K.; Noguchi, K.; Miyazawa, T.; Yui, T.; Ogawa, K. *Macromolecules* **1997**, *30*, 5849.
(26) Tadokoro, H. *Structure of Crystalline Polymers*; John Wiley & Sons: New York, 1979.
(27) www.Gaussian.com.
(28) Okada, K.; Noguchi, K.; Okuyama, K.; Arnott, S. *Comput. Biol. Chem.* **2003**, *27*, 265.
(29) *International Tables for X-ray Crystallography*; The Kynoch Press: Birmingham, 1979.
(30) Jeffrey, G. A. *Introduction to Hydrogen Bonding*; Oxford University Press: New York, 1997.

MA050161T